

Multiphoton Induced X-Ray Emission from Kr Clusters on M -Shell ($\sim 100 \text{ \AA}$) and L -Shell ($\sim 6 \text{ \AA}$) Transitions

A. McPherson, T. S. Luk, B. D. Thompson, A. B. Borisov, O. B. Shiryaev, X. Chen, K. Boyer, and C. K. Rhodes

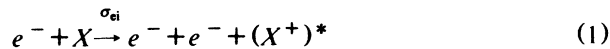
Laboratory for Atomic, Molecular, and Radiation Physics, Department of Physics, M/C 273, University of Illinois at Chicago, 845 W. Taylor, Room 2136, Chicago, Illinois 60607-7059

(Received 2 September 1993; revised manuscript received 28 December 1993)

Experiments demonstrating the role of cluster formation on multiphoton-induced x-ray emission and the scaling of this phenomenon into the kilovolt range have been performed on Kr. For the Kr M shell, augmentation of Kr_n formation leads to a large increase in Kr^{9+} ($4p \rightarrow 3d$) emission ($\sim 100 \text{ \AA}$) and the appearance of a strong band at $\sim 90 \text{ \AA}$. The observation of L -shell transitions ($\sim 5\text{--}7.5 \text{ \AA}$) demonstrates the scaling of this phenomenon into the kilovolt region and leads to the conclusion that the interaction produces direct inner-shell excitation with the emission of prompt x rays.

PACS numbers: 32.80.Wr, 32.30.Rj

It has been postulated [1] that a unified picture of high-intensity short-pulse multiphoton processes, embracing atoms, molecules, and solids, appears possible through the study of atomic and molecular clusters. Of particular significance in this analysis are *intracluster* processes involving inelastic electron collisions of the form



that can lead to the production of inner-shell excited species capable of prompt x-ray emission.

Essential predictions of the proposed model have been explicitly tested in new experimental studies involving five atomic shells [Kr(M), Kr(L), Xe(N), Xe(M), and Xe(L)]. This Letter establishes the crucial role of cluster formation in the generation of the anomalous emissions previously observed [2-4] from the Kr M shell ($\sim 110 \text{ eV}$) and demonstrates the scaling of this new phenomenon into the kilovolt range ($\sim 800\text{--}2100 \text{ eV}$) through measurements of Kr L -shell radiation.

The detection of intense Kr^{9+} ($4p \rightarrow 3d$) emission at $\sim 100 \text{ \AA}$ in earlier spectroscopic studies [2,3] using pulsed-gas targets presented an obvious paradox. Measurements of ion production [5] using tenuous gas targets, conducted under identical conditions of irradiation, had demonstrated that *no* production of Kr^{9+} was possible from free Kr atoms. Hence, the identification [6,7] of the Kr^{9+} emissions, produced by either a prompt or a delayed mechanism, was fully anomalous. However, if sufficient cluster formation were produced in the hydrodynamic flow of the jet furnishing the target [2-4], the cluster model showed that this paradox could be entirely resolved; the anomalous emissions found a simple explanation which applied generally to all cases considered [1].

The multiphoton-induced production of prompt short wavelength radiation from clusters requires that certain conditions be met [1]. These requirements establish relationships between the intensity of irradiation (I) and the cluster size (n) which define allowed zones for the emis-

sion to occur. Such emission can only take place if sufficient kinetic energy is possessed by the colliding electron in reaction (1) to excite an inner electron. This condition, based on a simple formulation of the work done by the external field on a free electron in the cluster, leads to the specification of two limiting intensities given by

$$I_0 = \frac{\epsilon_e^2}{8\pi\alpha n^{2/3} \hbar r_0^2}, \quad (2)$$

$$I_n(\lambda) = \frac{2\pi^3}{\alpha} \left(\frac{r_0}{\lambda} \right)^2 mc^2 \left(\frac{c}{\lambda_c} \right) \frac{n^{2/3}}{\lambda^2},$$

in which ϵ_e , r_0 , α , λ , m , λ_c , and c denote the inner-shell binding energy [8], the interatomic spacing, the fine structure constant, the wavelength of irradiation, the electron mass, the electron Compton wavelength, and the speed of light, respectively. Hence, an inner-shell $j-1$ electron with binding energy ϵ_e can be ionized if the intensity exceeds a *lower bound* given by either I_0 or $I_n(\lambda)$, whichever is greatest. In addition to the production of a vacancy in the $j-1$ shell, *prompt* $j \rightarrow j-1$ emission requires the retention of at least one electron in the outer j shell during the course of irradiation. This determines an *upper bound* on the intensity which, with the use of the tunneling ionization model [9], leads to a limiting intensity $I_{\max}(j)$ given by

$$I_{\max}(j) = cE_p^4(j)/128\pi e^6 Z^2, \quad (3)$$

where $E_p(j)$ is the ionization potential of the most tightly bound j -shell electron, Z the resulting ionic charge, and e the electronic charge. Hence, the allowed zones for prompt x-ray emission from atoms of a homonuclear cluster generally appear in the form shown for the Kr M and L shells in Fig. 1.

This picture leads to the prediction that an increase in the cluster density and average cluster size should lead to both a corresponding *intensification* and a spectral *modification* of the detected emission. Since Kr_n cluster formation can be strongly augmented by cooling the flow

in the jet [10,11], in light of the form of the allowed zone for the M shell in Fig. 1, a comparison of spectra observed at comparable pressures (densities) and substantially different temperatures should indicate the importance of the role of cluster species in the production of the radiating ions.

The experimental apparatus used has been described elsewhere [3]. The laser [12] employed in the present study, which had a wavelength of 248 nm, a pulse width of ~ 300 fs, and a power of ~ 0.7 TW, was focused with an $f/10$ CaF_2 lens into the gas target and provided a maximum focal intensity of $(0.5-1.0) \times 10^{17}$ W/cm^2 , conditions essentially the same as in the previous work [2-4]. The gas target was produced by a high-pressure pulsed valve fitted with a circular sonic nozzle having a diameter of 0.5 mm. The gas flow was cooled with free-flowing dry nitrogen which had passed through a liquid nitrogen bath. A thermocouple attached to the valve body measured the temperature of the gas and a grazing incidence spectrometer was used to record the spectra [2-4].

The relevant spectral comparison for Kr in the 72-112 Å region is presented in Fig. 2. The Kr spectrum illustrated in Fig. 2(a) was obtained with a stagnation pressure of 115 psia at 293 K, conditions very similar to those of the earlier work [2,3]. Figure 2(b) presents the Kr spectrum corresponding to a significantly reduced nozzle temperature (238 K) and a stagnation pressure (130 psia), nearly the same as that pertaining to the data in Fig. 2(a).

Three principal differences distinguish the spectra shown in Figs. 2(a) and 2(b). They are (1) a large increase in the observed Kr^{9+} ($4p \rightarrow 3d$) signal upon reduction of the temperature (e.g., from ~ 30 to ~ 450 at ~ 103 Å), (2) the appearance of a strong highly struc-

tured band at 90 Å at the lower temperature, and (3) the large relative reduction in Fig. 2(b) of the narrow features appearing in the 72-83 Å region of Fig. 2(a). Spectral data [6,7] indicate that the features observed in Fig. 2(b) in the 86-97 Å region arise from Kr^{10+} ($4p \rightarrow 3d$) transitions in the $\sim 86-91$ Å range and Kr^{9+} ($4s4p \rightarrow 4s3d$) lines in the $\sim 90-97$ Å interval. A contribution from $3p$ excitation in both Kr^{9+} and Kr^{10+} may occur in this same region. The spectrum also gives evidence for the presence of a broad unresolved band in the $\sim 76-85$ Å region composed of dense arrays [6] originating from Kr^{10+} ($4s4p \rightarrow 4s3d$) and Kr^{11+} ($4p \rightarrow 3d$) transitions.

These two signatures, a sharply increased signal strength and the appearance of new categories of transitions and higher charge states, are precisely the outcomes anticipated from enhanced cluster formation [1]. One expects that a higher cluster (Kr_n) density for fixed n would cause a corresponding increase in the emission and that the formation of larger clusters would lead to a further intensification of the emission and to new stages of ionization and classes of transitions. Since the 90 Å band only appeared in the cooled spectrum, we believe that it is mainly associated with the formation of the larger clusters produced at the lower temperature (238 K).

Figure 2(a) also exhibits the clear visibility of relatively weak narrow transitions in the $\sim 72-83$ Å region which can be associated with $4f \rightarrow 3d$ transitions [7] in Kr^{8+} . In distinct contrast to the lines in the 85-104 Å range, these features do *not* grow dramatically as the temperature is decreased. They remain weak and become relatively insignificant as the temperature is reduced. This sharply contrasting behavior indicates the action of a *different* mechanism for their excitation. Since the two spectra shown in Fig. 2 were generated under essentially the same *average* plasma conditions, conventional collisional mechanisms, such as recombination, should occur in largely the same fashion in both cases. This expectation matches the observed behavior of the transitions associated with $4f$ orbital excitation and we attribute those weak features to recombination.

The cluster model predicts the existence of large allowed regions associated with level structures in the kilovolt range, a property manifest in Fig. 1 through comparison of the zones associated with the M and L shells. Specifically, the model [1] predicts that the irradiation of Kr clusters with intensities above $\sim 10^{18}$ W/cm^2 , for nearly an arbitrary cluster distribution, should result in emission of prompt x rays from L -shell transitions [7, 13,14] in Kr ions (~ 7 Å).

Experiments testing this scaling behavior have been conducted with a peak intensity of $\sim 8 \times 10^{18}$ W/cm^2 . In this case, the focusing was provided by an $f/3$ off-axis parabolic mirror and a crystal spectrometer, using Kodak Industrex film and PET for the 4.5-7.5 range, was used.

The L -shell emission spectrum of Kr shown in Fig. 3, which involves transitions [7,13,14] from Kr^{q+} ($q=24-$

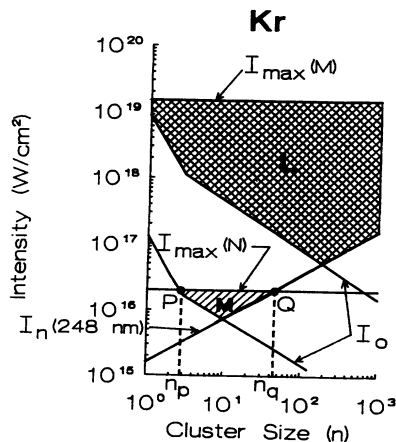


FIG. 1. Representation of the allowed zones for production of prompt Kr M - and L -shell emission from Kr clusters as a function of the intensity of 248 nm irradiation and cluster size. The boundaries outlining the allowed region are defined in the text. The maximum experimental intensities used for the M -shell and L -shell studies correspond to 1.0×10^{17} W/cm^2 and $\sim 8 \times 10^{18}$ W/cm^2 , respectively.

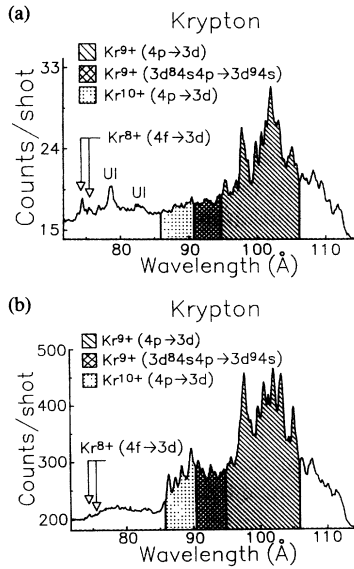


FIG. 2. Comparison of Kr spectra in the 72–112 Å region produced at different temperatures by multiphoton excitation with subpicosecond irradiation at 248 nm with a maximum intensity of $(0.5\text{--}1.0)\times 10^{17}$ W/cm². The vertical scales in both spectra are absolute values giving a valid measure of the comparative signal strengths. The spectral resolution is 0.9 ± 0.1 Å. (a) Nozzle temperature 293 K and stagnation pressure 115 psia. UI designates unidentified transitions. The base line corresponds to ~ 17 counts/shot. (b) Nozzle temperature 238 K and stagnation pressure 130 psia. Unresolved arrays from Kr¹⁰⁺ and Kr¹¹⁺ may contribute to the signal in the $\sim 76\text{--}85$ Å region.

27) in the 4.5–7.5 Å region, was recorded with 720 laser pulses. This spectrum exhibits several salient properties: (1) a group of strong $3l \rightarrow 2l'$ lines in the 6.3–7.7 Å region, (2) a small set of far weaker $4l, 5l \rightarrow 2p$ transitions in the 4.8–5.6 Å region, (3) lines with significant strength having $2s$ excitation (e.g., *F*), and (4) a substantial number of transitions involving satellite lines [14] [e.g., $Rk^{24+}(V/2p^6 3l3l' \leftarrow 2p^5 3d3l3l')$ and $Kr^{25+}(U/2p^6 3l \leftarrow 2p^5 3d3l)$ shown in the inset].

Several considerations bear directly on the interpretation of these data. First, the radiating charge states are anomalous. In analogy with the Kr⁹⁺ transitions discussed above, the presence of lines from Kr^{q+} ($q = 24\text{--}27$) is equally anomalous, since the tunneling ionization picture [5,9] predicts no charge states higher than Kr²²⁺. Second, the radiative transitions are fast. The lifetimes [15] of the $3s \rightarrow 2p$, $3d \rightarrow 2p$, and $3p \rightarrow 2s$ transitions occurring in the $\sim 6\text{--}7$ Å region fall largely in the 10–1000 fs range and the $2p \rightarrow 2s$ (~ 200 eV) transition [7] has a lifetime [16,17] less than 10 ps. Third, recombination and plasma collisional processes are relatively slow. Considering the properties of the flow, the relative positions of the focal zone and the nozzle, and the level of ionization ($Z \cong 25$), the maximum average electron density [4] is $\sim 5 \times 10^{20}$ cm⁻³. This gives a rate less

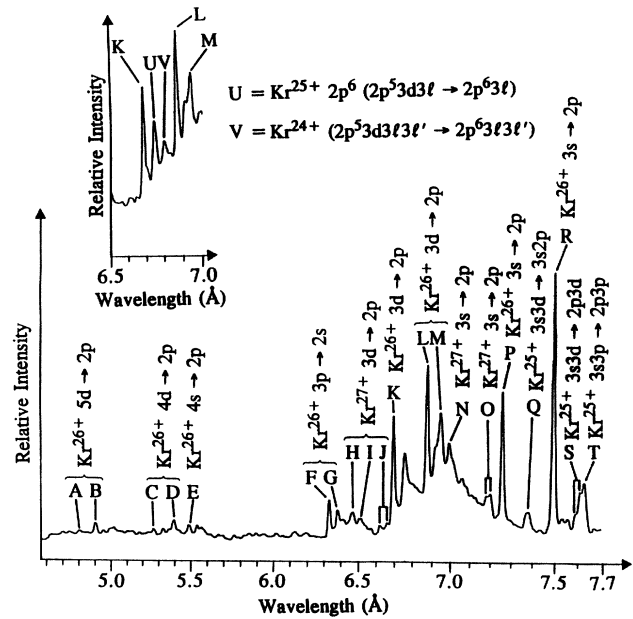


FIG. 3. Kr *L*-shell emission spectrum produced by multiphoton excitation with 248 nm radiation at a peak intensity of $\sim 8 \times 10^{18}$ W/cm². The stagnation pressure of the pulsed jet was 115 psia and the gas temperature was 243 K. Transitions from Kr^{q+} ($q = 24\text{--}27$) are identified. The inset, presenting data from another exposure, details the 6.5–7.0 Å region and shows the prominent Kr²⁴⁺ (*V*) and Kr²⁵⁺ (*U*) satellite lines observed in these experiments.

than 10^{10} s⁻¹ for both recombination [18] and $2s \rightarrow 2p$ collisional excitation [16].

In light of these considerations, the experimental observations lead to the following interpretations. The five weak transitions (*A–E*) associated with Kr²⁶⁺ all involve transitions of the form $nl \rightarrow 2p$ with $n \geq 4$. Since the *N*-shell limit [$I_{\max}(N)$] falls entirely below the allowed *L*-shell zone in Fig. 1, the postulated cluster mechanism cannot account for the presence of these lines. In analogy with the weak $4f \rightarrow 3d$ features occurring in Fig. 2(a), these lines are attributed to recombination from Kr²⁷⁺, a species identified by transitions (*H, I, J, N, O*).

The strong lines observed in the 6.3–7.7 Å region uniformly involve transitions with $3s$, $3p$, or $3d$ electrons. Using the most weakly bound of these ($3d$), and combining the information in Fig. 1 with the conditions for tunneling ionization [1,9], we can estimate the minimum cluster size necessary to observe *L*-shell ionization and still retain a $3d$ electron. Since the maximum intensity consistent with the retention of a $3d$ electron is $\sim 2 \times 10^{18}$ W/cm², the *L*-shell zone indicates that clusters with $n \geq 3$ would suffice. Evidence [10,11] on Kr_{*n*} formation indicates that an appreciable density with sizes at least as large as $n \sim 10$ is formed under our experimental conditions.

Lines *F* and *G* involve $2s$ excitation in Kr²⁶⁺. Since $2p \rightarrow 2s$ radiative decay is fast and electron collisional communication between the $2s$ and $2p$ states is slow, the

formation of $\text{Kr}^{26+} 2s2p^6 3p$ levels by recombination from excited $2s2p^6 \text{Kr}^{27+}$ ions would have to be rapid. However, since the plasma conditions cannot support a recombination rate comparable to the radiative decay, it follows that the Kr^{26+} excited states are *directly* produced in the excitation of the cluster. The same reasoning and conclusion hold in relation to the $3d \rightarrow 2p$ satellite lines [e.g., $\text{Kr}^{24+}(V)$ and $\text{Kr}^{25+}(U)$].

The comparison of the spectrum illustrated in Fig. 3 with corresponding data obtained with a Z pinch [13] reveals a relative abundance of satellite lines in the multiphoton spectrum and significant reversals in relative line intensities. Both observations are in natural accord with the cluster model. The strong appearance of satellite transitions in the multiphoton spectrum [e.g., $\text{Kr}^{24+}(V)$], at the relatively low average electron density characteristic of this experiment, is again indicative of a direct mechanism of production [1] in the cluster which can be associated with the existence of the allowed L-shell region. In the 6.3–7.7 Å region, the multiphoton ($m\gamma$) $3s \rightarrow 2p$ transitions consistently exhibit the anomalous property of having a greater intensity than the corresponding $3d \rightarrow 2p$ lines, while the reverse holds for the Z-pinch (Z) spectrum [13]. Specifically, for Kr^{26+} $R > L$ ($m\gamma$), $R < L$ (Z) and for Kr^{27+} $N > J$ ($m\gamma$), $N < J$ (Z). Recombining collisionally dominated optically thin plasmas characteristically produce emission with $nd \rightarrow 2p$ transitions dominating [19] the corresponding $ns \rightarrow 2p$ lines.

The anomalous strength of the $3s$ transitions congenially matches the expectations of the cluster picture. Electron loss can occur by tunneling ionization and intracluster inelastic electron collisions. With a maximum intensity of $8 \times 10^{18} \text{ W/cm}^2$, $3s$ electrons *cannot* be removed by the tunneling process [9], although the full $3d$ shell is ionized for intensities $> 2 \times 10^{18} \text{ W/cm}^2$. Collisionally, since the $3d$ ionization cross section [20,21] is approximately tenfold the value for the $3s$ level, retention of the $3s$ electron is again favored. It follows that in the region corresponding to L-shell excitation, particularly for intensities above $\sim 10^{18} \text{ W/cm}^2$, a higher probability exists for retention of $3s$ electrons than for $3d$. This tendency should also be enhanced for the higher charge states seen, assuming a greater intensity for their production. Namely, the $3s/3d$ ratio should be greater for Kr^{27+} than for Kr^{26+} , a feature that is reflected in the multiphoton data ($N/J > R/L$).

In summary, experimental studies of multiphoton-induced emissions in the 5–7.5 Å region from Kr have established that the cluster mechanism demonstrated in the ~ 80 –110 eV range scales into the kilovolt zone. The experimental evidence supports the conclusion that multiphoton coupling to clusters can *directly* generate inner-shell vacancies and the production of *prompt* x rays. Finally, recent measurements [22] demonstrating the multiphoton production of Xe(L) emission further corroborate this conclusion.

The authors acknowledge the expert technical assistance of J. Wright and P. Noel and extend special thanks to S. Guggenheim for the use of his densitometer. Helpful discussions are acknowledged (C.K.R.) with J. C. Solem, E. W. Schlag, K. Müller-Dethlefs, R. Jung, E. Waterstradt, H.-J. Dietrich, J. Belling, E. Grant, W. Sandner, U. Becker, J. Sugar, R. D. Cowen, R. B. Spielman, and R. E. Stewart. Support for this research was provided under Contracts No. (DOE) DE-FG02-91ER1208, No. AFOSR-89-0159, (ONR) No. N00014-91-J-1106, (SDI/NRL) No. N00014-91-K-2113, and (ARO) No. DAAL 3-91-G-0174. Partial support (C.K.R.) was provided by the Alexander von Humboldt Stiftung.

-
- [1] A. McPherson *et al.*, Appl. Phys. B **57**, 337 (1993).
 - [2] A. McPherson *et al.*, in *Fundamentals of Laser Interactions II*, edited by F. Ehlotzky (Springer-Verlag, Berlin, 1989), p. 93.
 - [3] A. McPherson *et al.*, J. Opt. Soc. Am. B **4**, 595 (1987).
 - [4] G. Gibson *et al.*, in *Short Wavelength Coherent Radiation: Generation and Applications*, edited by R. W. Falcone and J. Kirz (Optical Society of America, Washington, D.C., 1988), Vol. 2, p. 246.
 - [5] G. N. Gibson, T. S. Luk, and C. K. Rhodes, Phys. Rev. A **41**, 5049 (1990).
 - [6] L. A. Jones and E. Källne, J. Quant. Spectrosc. Radiat. Transfer **30**, 317 (1983).
 - [7] R. L. Kelley, J. Phys. Chem. Ref. Data **16**, Suppl. 1, 1 (1987).
 - [8] K.-N. Huang *et al.*, At. Data Nucl. Data Tables **18**, 243 (1976).
 - [9] S. Augst *et al.*, Phys. Rev. Lett. **63**, 2213 (1989).
 - [10] O. F. Hagena and W. Obert, J. Chem. Phys. **56**, 1793 (1972).
 - [11] S. T. Pratt and P. Dehmer, Chem. Phys. Lett. **87**, 533 (1982).
 - [12] B. Bouma *et al.*, J. Opt. Soc. Am. B **10**, 1180 (1993).
 - [13] R. B. Spielman *et al.*, J. Appl. Phys. **57**, 830 (1985).
 - [14] R. Stewart, *Experimental Studies of L-Shell X-Ray Emission from High Density Plasmas* (University Microfilms International, Ann Arbor, MI, 1985).
 - [15] P. G. Burkhalter *et al.*, J. Appl. Phys. **50**, 4532 (1979).
 - [16] G. A. Doschek and U. Feldman, J. Appl. Phys. **47**, 3083 (1976).
 - [17] W. L. Wiese, M. W. Smith, and B. M. Miles, in *Atomic Transition Probabilities* (U.S. GPO, Washington, D.C., 1969), NSRDS-NBS 22.
 - [18] D. R. Bates and A. Dalgarno, in *Atomic and Molecular Processes*, edited by D. R. Bates (Academic, New York, 1962), p. 245.
 - [19] H. A. Bethe and E. E. Salpeter, in *Quantum Mechanics of One- and Two-Electron Atoms* (Springer-Verlag, Berlin, 1957), p. 266.
 - [20] E. J. McGuire, Phys. Rev. A **16**, 73 (1977).
 - [21] C. J. Powell, Rev. Mod. Phys. **48**, 33 (1976).
 - [22] A. McPherson *et al.*, "Evidence for the Multiphoton Production of Hollow Atoms: Xe L-Shell Emission in the 4–5 keV Region" (to be published).

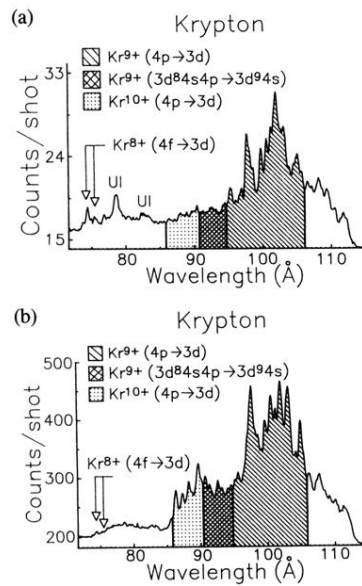


FIG. 2. Comparison of Kr spectra in the 72–112 Å region produced at different temperatures by multiphoton excitation with subpicosecond irradiation at 248 nm with a maximum intensity of $(0.5\text{--}1.0)\times 10^{17}$ W/cm². The vertical scales in both spectra are absolute values giving a valid measure of the comparative signal strengths. The spectral resolution is 0.9 ± 0.1 Å. (a) Nozzle temperature 293 K and stagnation pressure 115 psia. UI designates unidentified transitions. The base line corresponds to ~ 17 counts/shot. (b) Nozzle temperature 238 K and stagnation pressure 130 psia. Unresolved arrays from Kr¹⁰⁺ and Kr¹¹⁺ may contribute to the signal in the $\sim 76\text{--}85$ Å region.